Cell Reports, Volume *40*

Supplemental information

Skeletal progenitors preserve proliferation and self-renewal upon inhibition of mitochondrial respiration by rerouting the TCA cycle

Guillaume Tournaire, Shauni Loopmans, Steve Stegen, Gianmarco Rinaldi, Guy Eelen, Sophie Torrekens, Karen Moermans, Peter Carmeliet, Bart Ghesquière, Bernard Thienpont, Sarah-Maria Fendt, Nick van Gastel, and Geert Carmeliet

Figure S1

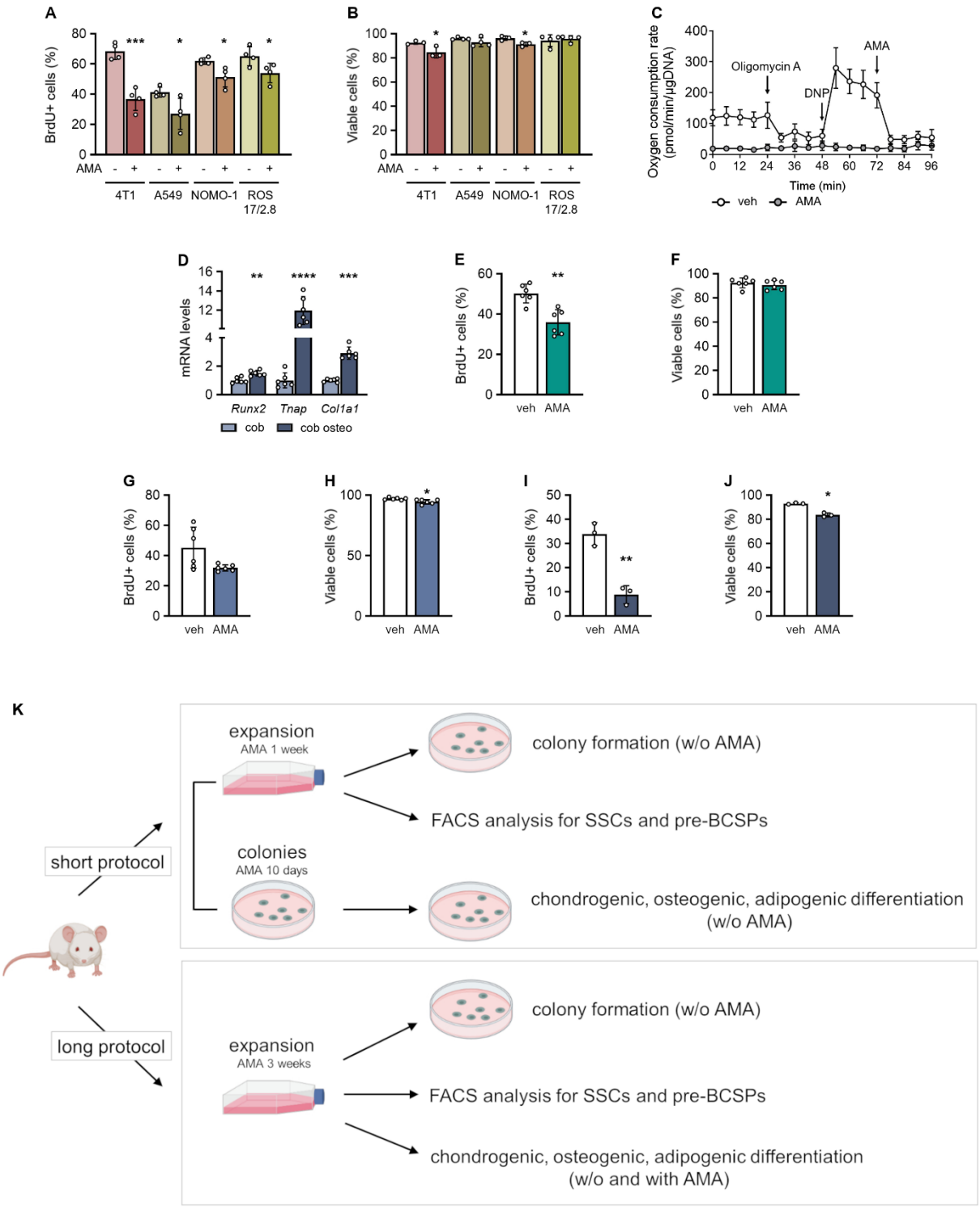
A
BrdU+ cells (%)
AMA
4T1
A549
NOMO-1
ROS 17/2.8
B
Viable cells (%)
C
Oxygen consumption rate (pmol/min/µgDNA)
Oligomycin A
DNP
AMA
Time (min)
veh
AMA
D
mRNA levels
Runx2
Tnap
Col1a1
cob
cob osteo
E
F
G
H
I
J
K
expansion
AMA 1 week
colony formation (w/o AMA)
FACS analysis for SSCs and pre-BCSPs
colonies
AMA 10 days
chondrogenic, osteogenic, adipogenic differentiation (w/o AMA)
short protocol
long protocol
expansion
AMA 3 weeks
colony formation (w/o AMA)
FACS analysis for SSCs and pre-BCSPs
chondrogenic, osteogenic, adipogenic differentiation (w/o and with AMA)

Figure S1. Effect of AMA on tumor cell lines and periosteal cells and strategy to investigate the effect of AMA on SSPC properties, related to Figure 1.
(A) Flow cytometry analysis of BrdU positive ($BrdU^+$) 4T1, A549, NOMO-1and ROS 17/2.8 cancer cells treated with vehicle (veh) or 10µM Antimycin A (AMA) for 7 days (n=4).
(B) Cell viability, using Annexin V-Propidium Iodide flow cytometry, of 4T1, A549, NOMO-1and ROS 17/2.8 cancer cells treated with veh or AMA for 7 days (n=3-4).
(C) Oxygen consumption rate in veh- and AMA-treated mouse periosteal cells (2,4-dinitrophenol, DNP; n=3).
(D) Culturing calvarial osteoblasts (cob) for 3 days in osteogenic differentiation medium (cob osteo) results in mature osteoblasts, assessed by quantification of *Runx2*, *Tnap* and *Col1a1* mRNA levels (n=6).
(E) Flow cytometry analysis of $BrdU^+$ growth plate chondrocytes treated with veh or 10µM AMA for 24h (n=6).
(F) Cell viability, using Annexin 0V-Propidium Iodide flow cytometry, of growth plate chondrocytes treated with veh or AMA for 24h (n=6).
(G) Flow cytometry analysis of $BrdU^+$ calvarial cells treated with veh or AMA for 24h (n=6).
(H) Cell viability, using Annexin V-Propidium Iodide flow cytometry, of calvarial cells treated with veh or AMA for 24h (n=6).
(I) Flow cytometry analysis of $BrdU^+$ mature osteoblasts (cob osteo) treated with veh or 10µM AMA for 24h (n=3).
(J) Cell viability, using Annexin V-Propidium Iodide flow cytometry, of mature osteoblasts (cob osteo) treated with veh or AMA for 24h (n=3).
(K) Schematic representation of experimental design to investigate SSPC properties. The effect of AMA treatment on SSPC properties was determined using a short or long protocol. In the short protocol, periosteal cells were expanded for 1 week with vehicle or AMA and their capacity to form colonies, in the absence of AMA, as well as the percentage of skeletal stem cells (SSCs) and pre-bone, cartilage and stromal progenitors (pre-BCSPs) was investigated. In parallel, freshly isolated cells were seeded at clonal density and treated with AMA for 10 days. AMA treatment was stopped and colonies were further cultured in medium inducing chondrogenic, osteogenic or adipogenic differentiation to investigate their tri-lineage potential.
In the long protocol, we expanded cells for 3 weeks, corresponding to 3 passages, with vehicle or AMA and analyzed their capacity to form colonies, the percentage of SSCs and pre-BCSPs and their tri-lineage differentiation potency in the presence or absence of AMA.
Data are means ± SD. *$p<0.05$, **$p<0.01$, ***$p<0.001$, ****$p<0.0001$ vs veh (two-tailed Student's *t*-test).

Figure S2

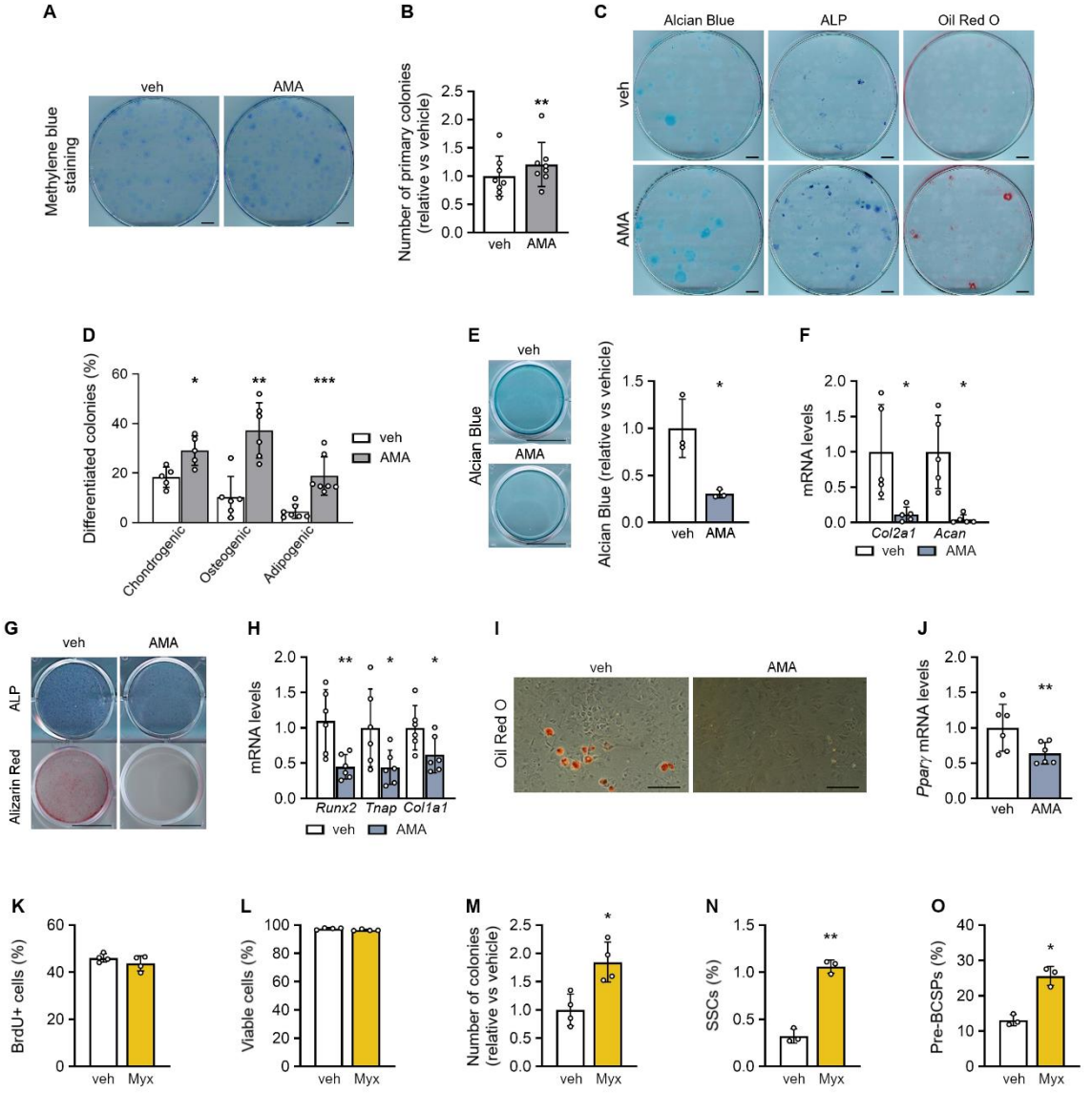

Figure S2. AMA treatment during expansion of SSPCs preserves their multilineage potential, but has negative effects when used during differentiation, related to Figure 1.
(A and B) Visualization (A, Methylene blue staining) and quantification of the number of colonies formed after culture of SSPCs with vehicle (veh; control) or 10µM Antimycin A (AMA) for 10 days (B, n=8).
(C and D) Visualization of chondrogenic, osteogenic and adipogenic differentiation of colonies (C) and quantification of the number of colonies (D) staining positive respectively for the presence of chondrogenic matrix (Alcian blue; n=5), alkaline phosphatase activity (ALP; n=6) or lipid deposits (Oil Red O; n=7). Colonies were formed in the presence of veh or AMA, but differentiated in the absence of AMA.
(E and F) Chondrogenic differentiation in the presence of veh (control) or AMA, assessed by visualization and quantification of chondrogenic matrix deposition (Alcian blue staining) (E; n=3) and quantification of *Col2a1* and *Acan* mRNA levels (F; n=5).
(G and H) Osteogenic differentiation in the presence of veh or AMA, assessed by visualization of alkaline phosphatase activity (ALP) and mineralized matrix deposition (Alizarin red staining) (G; n=3) and quantification of *Runx2*, *Tnap*, *Col1a1* mRNA levels (H; n=6).
(I and J) Adipogenic differentiation in the presence of veh or AMA, assessed by visualization of lipid deposits (Oil Red O staining) (I; n=4) and quantification of *Pparγ* mRNA levels (J; n=6).
(K) Flow cytometry analysis of $BrdU^+$ SSPCs treated with veh or 10µM Myxothiazol (Myx) for 7 days (n=4).
(L) Cell viability, using Annexin V-Propidium Iodide flow cytometry, of SSPCs treated with veh or Myx (n=4).

(M) Number of colonies formed after culture of SSPCs with veh (control) or Myx (n=4).
(N and O) Flow cytometry analysis of the percentage of skeletal stem cells (SSCs, N) and pre-bone, cartilage and stromal progenitors (pre-BCSPs, O) in veh- or Myx-treated cells (n=3).
Data are means ± SD. *p<0.05, **p<0.01, ***p<0.001 vs veh (paired two-tailed Student's *t*-test). Scale bar in A, C, E, G: 1 cm; in I: 200 μm.

Figure S3

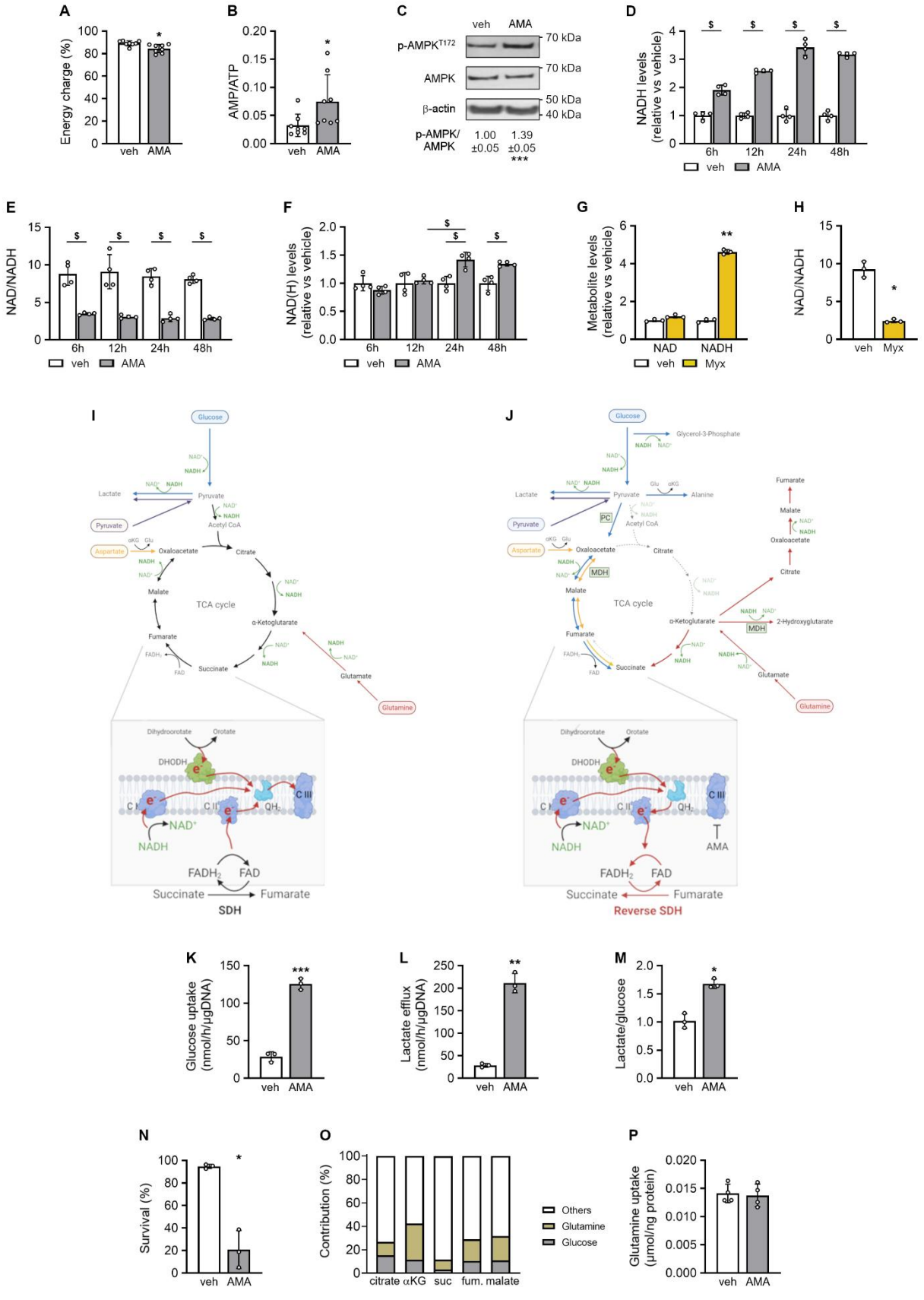
A
Energy charge (%)
veh AMA
B
AMP/ATP
veh AMA
C
veh AMA
p-AMPK^{T172}
AMPK
β-actin
70 kDa
70 kDa
50 kDa
40 kDa
p-AMPK/ AMPK
1.00 ±0.05
1.39 ±0.05
***
D
NADH levels (relative vs vehicle)
6h 12h 24h 48h
veh AMA
E
NAD/NADH
6h 12h 24h 48h
veh AMA
F
NAD(H) levels (relative vs vehicle)
6h 12h 24h 48h
veh AMA
G
Metabolite levels (relative vs vehicle)
NAD NADH
veh Myx
H
NAD/NADH
veh Myx
I
Glucose
Lactate
Pyruvate
Acetyl CoA
Aspartate
Oxaloacetate
Citrate
Malate
TCA cycle
α-Ketoglutarate
Fumarate
Succinate
Glutamate
Glutamine
Dihydroorotate
Orotate
DHODH
C I
C II
C III
QH$_2$
NAD$^+$
NADH
FADH$_2$
FAD
Succinate
Fumarate
SDH
J
Glycerol-3-Phosphate
Alanine
PC
MDH
2-Hydroxyglutarate
Reverse SDH
AMA
K
Glucose uptake (nmol/h/μgDNA)
veh AMA
L
Lactate efflux (nmol/h/μgDNA)
veh AMA
M
Lactate/glucose
veh AMA
N
Survival (%)
veh AMA
O
Contribution (%)
citrate αKG suc fum. malate
Others
Glutamine
Glucose
P
Glutamine uptake (μmol/ng protein)
veh AMA

Figure S3. SSPCs are in energy stress despite increased glycolysis and they increase the NAD(H) pool to preserve proliferation upon ETC inhibition, related to Figure 2.

(A and B) Energy charge calculated as ([ATP] + ½ [ADP])/([ATP]+ [ADP]+ [AMP]) (A; n=8) and AMP to ATP ratio (B; n=8) in cells treated with vehicle (veh) or 10μM Antimycin A (AMA).

(C) Immunoblot of p-AMPK^{T172}, AMPK, and β-actin with quantification of p-AMPK^{T172} to AMPK ratio in veh- and AMA-treated cells. Representative images of 3 experiments are shown.

(D-F) NADH levels (D; n=4), NAD/NADH ratio (E; n=4) and NAD + NADH (NAD(H)) levels (F; n=4) in cells treated with veh (control) or AMA for indicated time points.

(G and H) NAD and NADH levels (G; n=3) and NAD/NADH ratio (H; n=3) in cells treated with veh (control) or 10μM Myxothiazol (Myx) for 3 days.

(I) Schematic representation showing pathways that produce NADH in veh-treated cells or that regenerate NAD^+ by converting pyruvate to lactate and by transferring electrons (e^-) to the electron transfer chain (ETC). (DHODH: dihydroorotate dehydrogenase; C I: complex I of ETC; C II: complex II; C III: complex III; QH_2: ubiquinol; SDH: succinate dehydrogenase)

(J) Schematic representation showing metabolic adaptations in AMA-treated cells: pathways producing NADH are downregulated, including pyruvate dehydrogenase (PDH) and the conversion of citrate to □-ketoglutarate in the TCA cycle, while pathways that can regenerate NAD^+ are stimulated, including the conversion of glucose to glycerol-3-phosphate, of α-Ketoglutarate to 2-Hydroxyglutarate and of Oxaloacetate to Malate. In addition, reverse SDH activity allows that electrons are still transferred from C I and DHODH to QH2. Thin dashed arrows indicate downregulation (Glu: Glutamate; αKG, α-Ketoglutarate; MDH: malate dehydrogenase).

(K-M) Glucose uptake (K; n=3), lactate efflux (L; n=3) and ratio of lactate efflux to glucose uptake (M; n=3) in veh- and AMA-treated cells.

(N) Cell viability of veh- and AMA-treated cells cultured for 24h in glucose-deprived medium (0,5mM) and analyzed by Annexin V-Propidium Iodide flow cytometry (n=3).

(O) Fractional contribution of $^{13}C_5$-glutamine and $^{13}C_6$-glucose to citrate, αKG, succinate (suc), fumarate (fum) and malate in periosteal cells (n=8).

(P) Consumption of glutamine during 24h by veh- and AMA-treated cells (n=4).

Data are means ± SD. *p<0.05, **p<0.01, ***p<0.001 vs veh (paired two-tailed Student's *t*-test), $^{\$}$p<0.05 (two-way ANOVA).

Figure S4

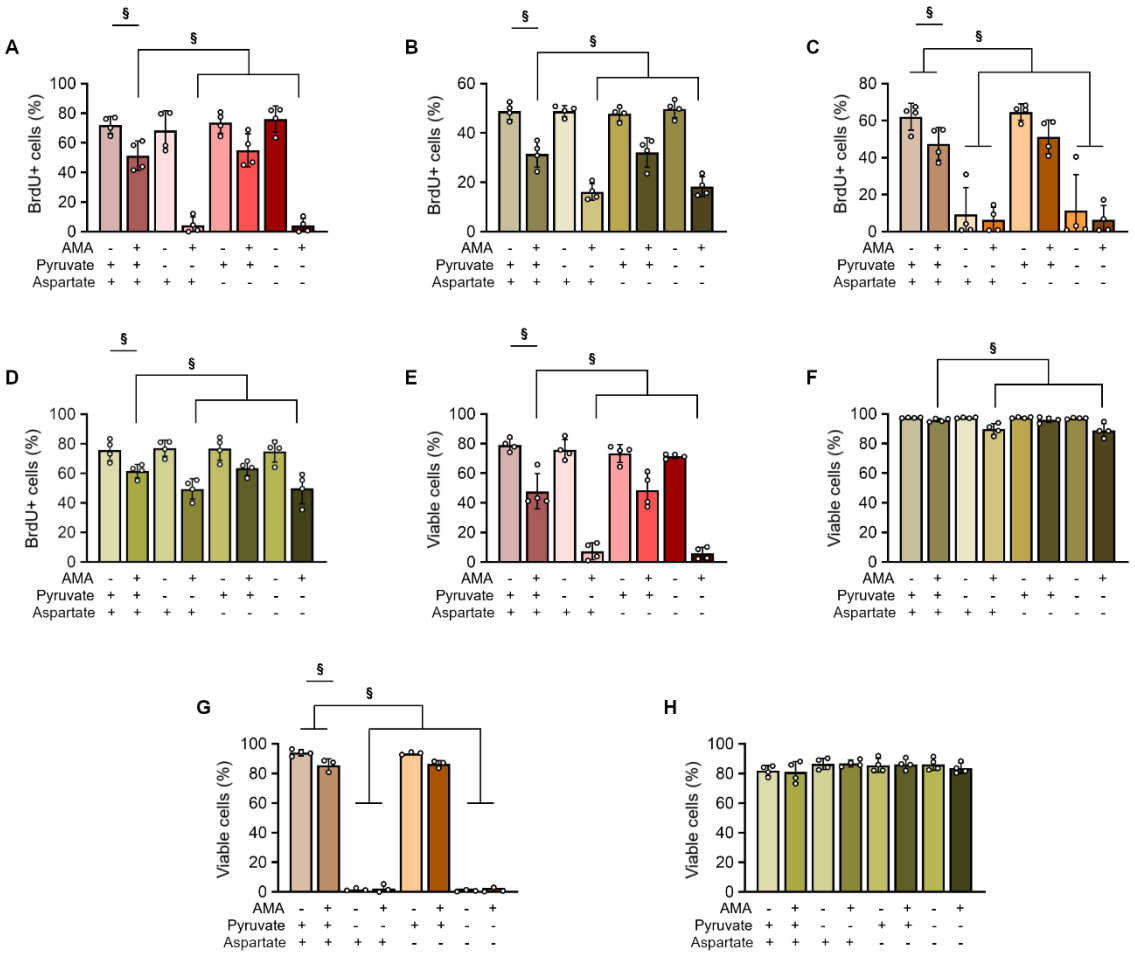

Figure S4. Tumor cells rely on pyruvate upon AMA-treatment, related to Figure 3.
(A-D) Flow cytometry analysis of BrdU positive ($BrdU^+$) 4T1 (A; n=4), A549 (B; n=4), NOMO-1 (C; n=4) and ROS 17/2.8 (D; n=4) cancer cells treated with vehicle (veh) or 10µM Antimycin A (AMA) for 7 days and then for 24h in medium with 1mM pyruvate and 0.22mM aspartate or without pyruvate and/or aspartate.
(E-H) Cell viability, using Annexin V-Propidium Iodide flow cytometry, of 4T1 (E; n=4), A549 (F; n=4), NOMO-1 (G; n=3) and ROS 17/2.8 (H; n=4) cancer cells treated with veh or 10µM AMA for 7 days and then for 24h in medium with 1mM pyruvate and 0.22mM aspartate or without pyruvate and/or aspartate.
Data are means ± SD. $^{§}p<0.05$ (three-way ANOVA).

Figure S5

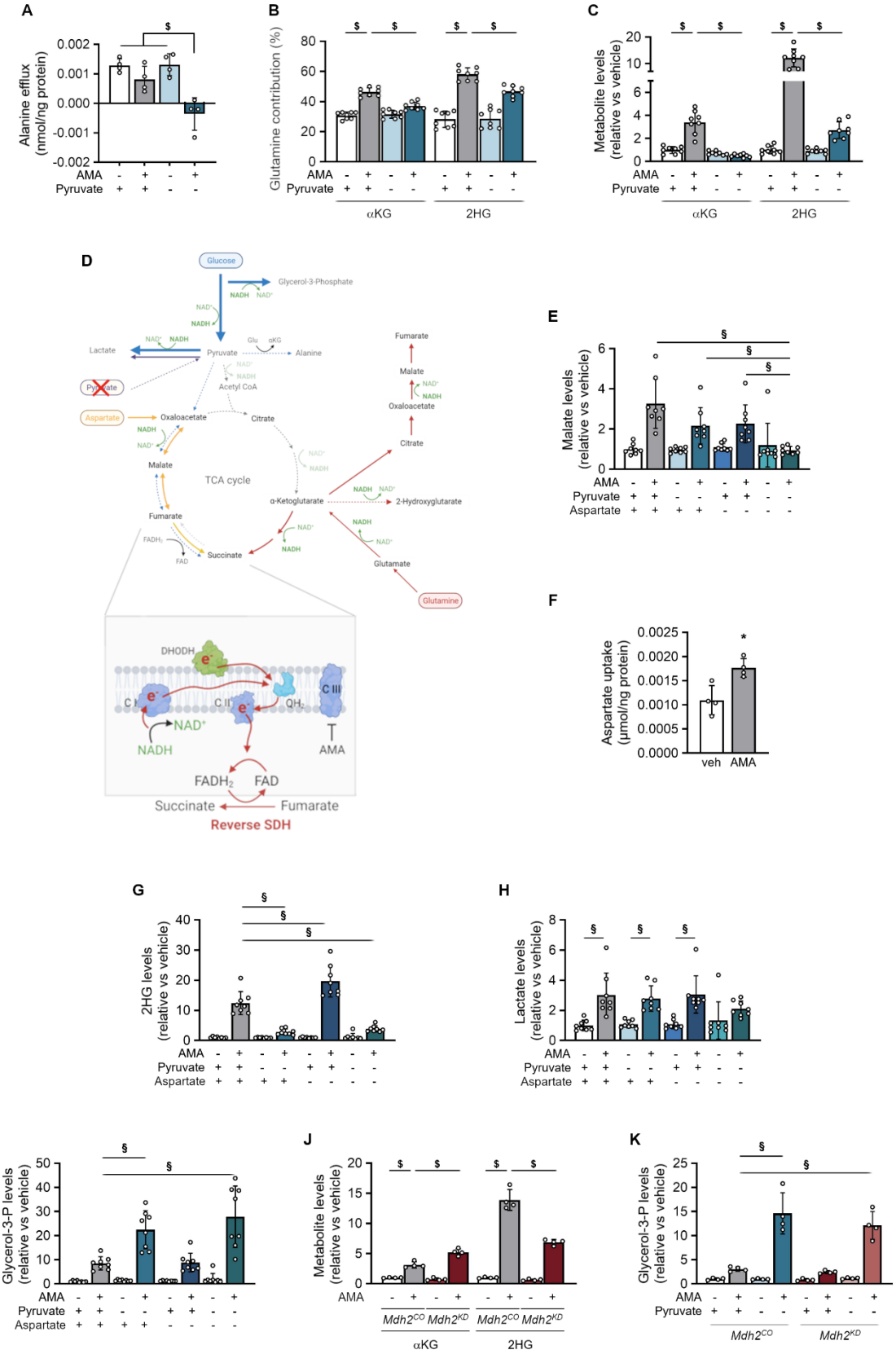
A
Alanine efflux (nmol/ng protein)
AMA
Pyruvate
B
Glutamine contribution (%)
αKG
2HG
C
Metabolite levels (relative vs vehicle)
D
Glucose
Glycerol-3-Phosphate
Lactate
Pyruvate
Alanine
Acetyl CoA
Aspartate
Oxaloacetate
Citrate
Malate
TCA cycle
Fumarate
α-Ketoglutarate
2-Hydroxyglutarate
Succinate
Glutamate
Glutamine
DHODH
C I
C II
C III
QH2
NAD+
NADH
FADH2
FAD
AMA
Succinate
Fumarate
Reverse SDH
E
Malate levels (relative vs vehicle)
Aspartate
F
Aspartate uptake (µmol/ng protein)
veh
AMA
G
2HG levels (relative vs vehicle)
H
Lactate levels (relative vs vehicle)
I
Glycerol-3-P levels (relative vs vehicle)
J
Metabolite levels (relative vs vehicle)
Mdh2CO
Mdh2KD
K
Glycerol-3-P levels (relative vs vehicle)

Figure S5: Extracellular pyruvate and aspartate promote NAD^+ regeneration, related to Figure 3.
(A) Alanine efflux during 24h by cells treated with vehicle (veh) or 10μM Antimycin A (AMA) (n=4)
(B) Fractional contribution of $^{13}C_5$-glutamine to α-ketoglutarate (αKG) and 2-hydroxyglutarate (2HG) in veh- and AMA-treated cells cultured with or without 1mM pyruvate (n=8)
(C) αKG and 2HG levels in veh (control)- and AMA-treated cells cultured with or without pyruvate (n=8).
(D) Schematic representation of metabolic adaptations in AMA-treated cells cultured in pyruvate-deprived condition. Pyruvate deprivation decreases the contribution of glucose to malate and the conversion of glucose to alanine, thereby reducing the production of αKG and indirectly of 2HG, which could affect NAD^+ regeneration. NAD^+ levels are nevertheless maintained by increased glucose contribution to glycerol-3-phosphate (glycerol-3-P). Thick arrows indicate upregulation, thin dashed arrows downregulation.
(E) Malate levels in veh (control)- and AMA-treated cells cultured in medium with 1mM pyruvate and 0.22mM aspartate or without pyruvate and/or aspartate (n=8).
(F) Aspartate consumption during 24h by veh- and AMA-treated cells (n=4).
(G-I) 2HG (G), Lactate (H) and glycerol-3-P(I) levels in veh (control)- and AMA-treated cells cultured in medium with 1mM pyruvate and 0.22mM aspartate or without pyruvate and/or aspartate (n=8).
(J) αKG and 2HG levels in veh (control)- and AMA-treated cells transduced with control ($Mdh2^{CO}$) or MDH2-specific shRNA ($Mdh2^{KD}$) (n=4).
(K) Glycerol-3-P levels in veh (control)- and AMA-treated $Mdh2^{CO}$ and $Mdh2^{KD}$ cells cultured with or without pyruvate (n=4).
Data are means ± SD. *p<0.05 (paired two-tailed Student's *t*-test), $^{\$}$p<0.05 (two-way ANOVA), §p<0.05 (three-way ANOVA).

Figure S6

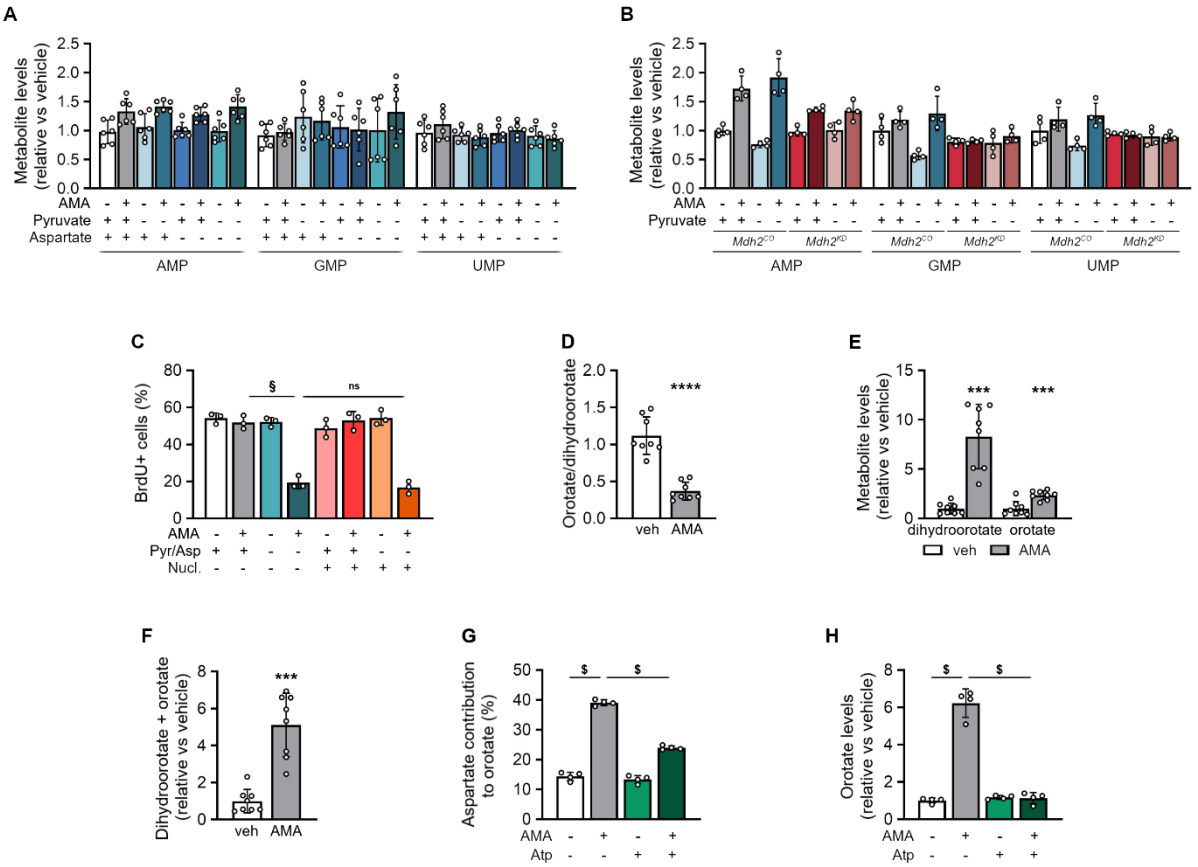

Figure S6. DHODH activity is preserved allowing pyrimidine synthesis, related to Figure 3.
(A and B) AMP, GMP and UMP levels in cells treated with vehicle (veh; control) or 10μM Antimycin A (AMA), cultured in medium with 1mM pyruvate and 0.22mM aspartate or without pyruvate and/or aspartate (A; n=6) or in veh- and AMA-treated cells transduced with control (*Mdh2*^{CO}) or MDH2-specific shRNA (*Mdh2*^{KD}) and cultured with or without pyruvate (B; n=4).
(C) Flow cytometry analysis of BrdU positive (BrdU^{+}) cells, treated with veh or AMA and cultured in full or pyruvate/aspartate (Pyr/Asp)-deprived medium supplemented or not with nucleosides (Nucl. n=3).
(D-F) Orotate to dihydroorotate ratio (D; n=8), dihydroorotate and orotate levels (E; n=8) and dihydroorotate + orotate pool (F; n=8) in veh (control)- and AMA-treated cells.
(G and H) Fractional contribution of $^{13}C_4$-aspartate to orotate (H; n=4) and orotate levels (I; n=4) in cells treated with veh (control), 10μM AMA and/or 500nM Atpenin A5 for 3 days.
Data are means ± SD. ***p<0.001, ****p<0.0001 vs veh (paired two-tailed Student's *t*-test), ns is not significant; $^{\$}$p<0.05 (two-way ANOVA), §p<0.05 (three-way ANOVA).

Figure S7

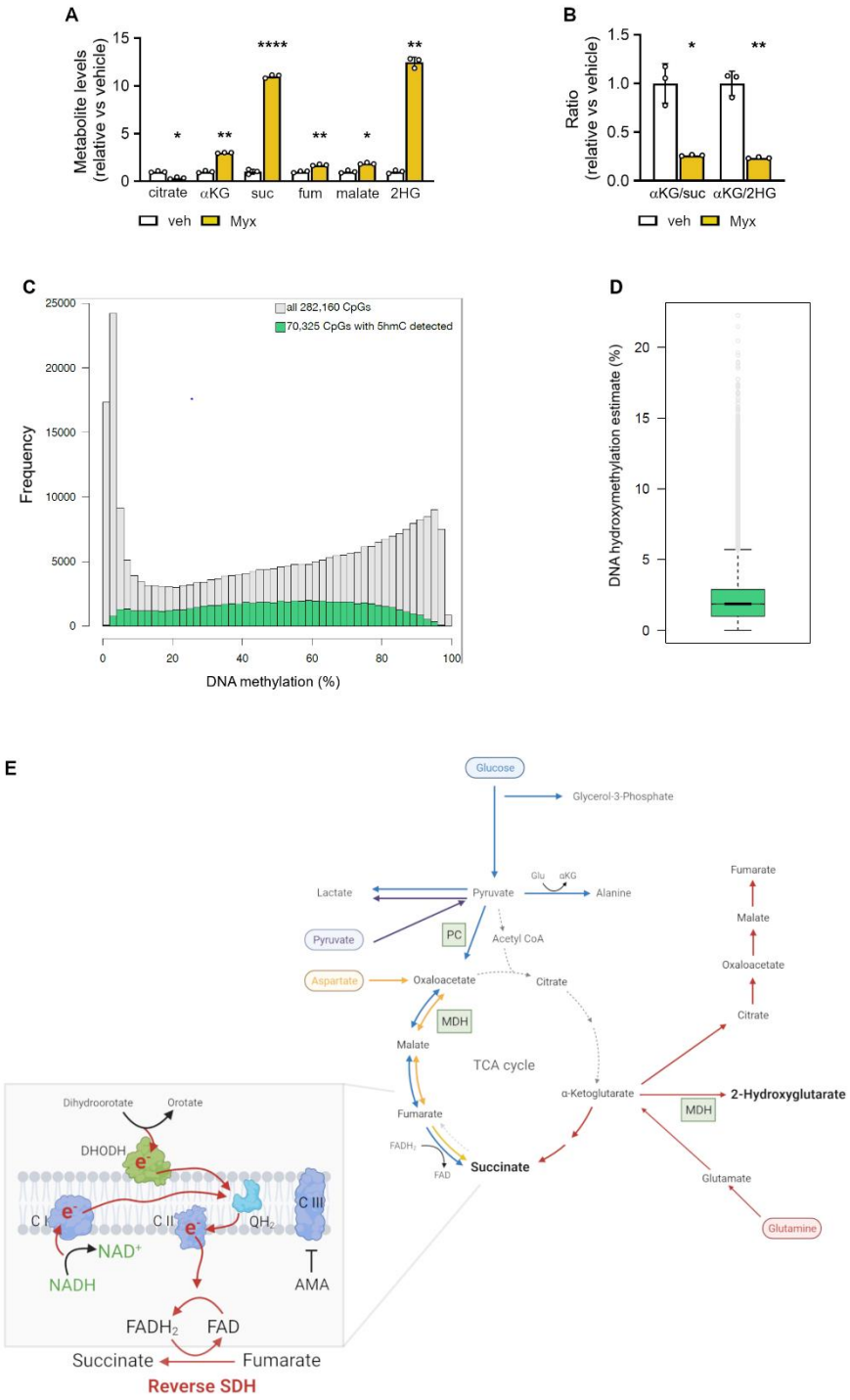
A
Metabolite levels (relative vs vehicle)
citrate
αKG
suc
fum
malate
2HG
veh
Myx
B
Ratio (relative vs vehicle)
αKG/suc
αKG/2HG
C
all 282,160 CpGs
70,325 CpGs with 5hmC detected
Frequency
DNA methylation (%)
D
DNA hydroxymethylation estimate (%)
E
Glucose
Glycerol-3-Phosphate
Lactate
Pyruvate
Alanine
PC
Acetyl CoA
Aspartate
Oxaloacetate
Citrate
MDH
Malate
TCA cycle
Fumarate
α-Ketoglutarate
2-Hydroxyglutarate
Succinate
Glutamate
Glutamine
Dihydroorotate
Orotate
DHODH
C I
C II
C III
NAD+
NADH
AMA
FADH2
FAD
Reverse SDH

Figure S7: Altered metabolite levels affect DNA demethylation, related to Figure 5.
(A and B) Citrate, α-ketoglutarate (αKG) succinate (suc), fumarate (fum), malate and 2-hydroxyglutarate (2HG) levels (A; n=3) and ratios of αKG to suc and of αKG to 2HG (B; n=3) in cells treated with vehicle (veh; control) or 10μM Myxothiazol (Myx) for 3 days.
(C) Histogram showing total DNA methylation and 5hmC signal among all 282,160 CpGs investigated.
(D) 5hmC levels in the 70,325 CpGs showing a 5hmC signal.
(E) Schematic representation of the metabolic adaptations upon ETC inhibition that result in increased levels of succinate and 2HG relative to αKG, which may induce TET activity that results in preservation of SSPC properties. Glutamine-derived αKG is converted to 2HG by malate dehydrogenase (MDH) or metabolized in the TCA cycle to succinate. Succinate cannot be further converted to fumarate as succinate dehydrogenase (SDH) is indirectly blocked by ETC complex III inhibition. Glucose-derived pyruvate enters the TCA cycle via pyruvate carboxylase (PC) and is further converted by MDH to malate and then by reverse SDH to succinate. Aspartate is also converted to succinate by the same pathway.
Data are means ± SD. *p<0.05, **p<0.01, ****p<0.0001 vs veh (two-tailed Student's *t*-test).

Table S1: List of chemicals. Related to STAR Methods: cell culture, treatment conditions.

Compounds	Supplier	Catalog number	Concentration
AKB	Sigma-Aldrich	Cat# K401	1mM
Antimycin A	Sigma-Aldrich	Cat# A8674	10µM
Aspartate	Sigma-Aldrich	Cat# A9256	0.2mM
Atpenin A5	Enzo	Cat# ALX-380-313	500nM
FK866	Sigma-Aldrich	Cat# F8557	10nM
L-Ascorbic Acid	Sigma-Aldrich	Cat# A4544	0.5mM
Myxothiazol	Sigma-Aldrich	Cat# T5580	10µM
Nucleoside mixture	merck millipore	Cat# ES-008-D	x1
Cytidine	-	-	0.73g/L
Guanosine	-	-	0.85g/L
Uridine	-	-	0.73g/L
Adenosine	-	-	0.8g/L
Thymidine	-	-	0.24g/L
Pyruvate	Gibco	Cat# 11360-039	1mM

Table S2: List of oligonucleotides. Related to STAR Methods: RNA extraction and qRT-PCR.

Short hairpins sequences			
gene	**Sequence**		
sh*Mdh2*	CCGGCGGAATGCACTTACTTCTCTACTCGAGTAGAGAAGTAAGTGCATTCCGTTTTTG		
qRT-PCR primers			
gene	**forward primer**	**probe**	**reverse primer**
Alp	CGCACGCGATGCAACA	CACTCAGGGCAATGAGGTCACATCCA	CGGACTTCCCAGCATCCTT
Coll1a1	TGTCCCAACCCCCAAAGAC	ACGTATTCTTCCGGGCAGAAAGCACA	CCCTCGACTCCTACATCTTCTGA
Coll2a1	AGAACATCACCTACCACTGTAAGAACA	CCTTGCTCATCCAGGGCTCCAATG	TGACGGTCTTGCCCCACTT
Mdh2	GAAGGAGTCGTTGAGTGTTCTT	-	CCAATGCCCAGGTTCTTCT
Nampt	TGG TTA CAG AGG AGT CTC TTC G	-	AAG CCG TTA TGG TAC TGT GC
Pcx	TGAGGCTCCTGGGTGTC	-	GATGGCAATCTCACCTCTGTT
Pparγ	CCCAATGGTTGCTGATTACAAA	CTGAAGCTCCAAGAATACCAAAGTGCGATC	AATAATAAGGTGGAGATGCAGGTTCT
Runx2	TACCAGCCACCGAGACCAA	CTTGTGCCCTCTGTTGTAAATACTGCTTGCA	AGAGGCTGTTTGACGCCATAG
Sox9	TCTGGAGGCTGCTGAACGA	CAGCACAAGAAAGACCACCC	TCCGTTCTTCACCGACTTCCT
Tet1	CAGCCGTTGAAATACATGCTC	-	ACATCCCACAGACCGAAGA
Tet2	AGAGCCTCAAGCAACCAAAA	-	ACATCCCTGAGAGCTCTTGC
Tet3	CCTTTTCTCCATACCGATCCTC	-	GAGTTCCCTACCTGCGATTG

Table S3: List of antibodies used for immunofluorescence and flow cytometry analysis. Related to STAR Methods: Western blot, Flow cytometry analysis and cell sorting.

	Antigen/reagent	Host	Conjugate	Supplier	Catalog number	Dilution
Primary antibodies	5hmc	Rabbit	-	Active Motif	39769	1/10000
	AMPKα	Rabbit	-	Cell Signaling Technology	2532	1/1000
	β-actin	Mouse	-	Sigma-Aldrich	A5441	1/10000
	BP1	Rat	PE	eBioscience	12-5891-81	1/200
	CD31	Rat	-	BD Biosciences	550274	1/50
	CD31	Rat	APC	eBioscience	17-0311-80	1/500
	CD45	Rat	APC	eBioscience	17-0451-83	1/500
	CD51	Rat	Biotin	eBioscience	13-0512-82	1/200
	CD90.2	Rat	PE	eBioscience	12-0903-81	1/200
	CD105	Rat	PE	eBioscience	12-1051-81	1/40
	CD200	Rat	PerCP-eFluor 710	eBioscience	46-5200-82	1/200
	HIF1α	Rabbit	-	Novus Biologicals	NB100-449	1/1000
	GFP	Rabbit	-	Invitrogen	A11122	1/200
	Histone H3	Rabbit	-	Cell Signaling Technology	4499	1/2000
	Histone H3 (di methyl K9)	Rabbit	-	Abcam	ab176882	1/1000
	Histone H3 (tri methyl K27)	Rabbit	-	Abcam	ab192985	1/1000
	Histone H3 (di methyl K79)	Rabbit	-	Abcam	ab3594	1/1000
	Lamin A/C	Goat	-	Santa Cruz	sc-6215	1/1000
	Mdh2	Rabbit	-	Abcam	ab96193	1/1000
	Osterix	Rabbit	-	Santa Cruz	sc-22536-R	1/10000
	PC	Rabbit	-	Invitrogen	PA5-50101	1/1000
	Phospho-AMPKα	Rabbit	-	Cell Signaling Technology	2535	1/1000
	Ter119	Rat	APC	eBioscience	17-5921-83	1/200
Secondary antibodies	anti-Goat	Rabbit	HRP	Dako	P0160	1/5000
	anti-Mouse	Rabbit	HRP	Dako	P0161	1/5000
	anti-Rabbit	Goat	Alexa 546	Invitrogen	A11010	1/200
	anti-Rabbit	Goat	Alexa 488	Invitrogen	A11008	1/200
	anti-Rabbit	Goat	HRP	Dako	P0448	1/5000
	anti-Rat	Goat	Biotin	BD Biosciences	559286	1/100
	Streptavidin	-	PE-Cyanine7	eBioscience	25-4317-82	1/200